AGU PUBLICATIONS

Geophysical Research Letters

RESEARCH LETTER
10.1002/2014GL061493

Key Points:
- The nearly uniform magnetic field is important to the dayside chorus excitation
- A small magnetic field inhomogeneity lowers the threshold free energy

Correspondence to:
X. Tao,
xtao@ustc.edu.cn

Citation:
Tao, X., Q. Lu, S. Wang, and L. Dai (2014), Effects of magnetic field configuration on the day-night asymmetry of chorus occurrence rate: A numerical study, *Geophys. Res. Lett.*, *41*, 6577–6582, doi:10.1002/2014GL061493.

Received 10 AUG 2014
Accepted 10 SEP 2014
Accepted article online 16 SEP 2014
Published online 2 OCT 2014

Effects of magnetic field configuration on the day-night asymmetry of chorus occurrence rate: A numerical study

X. Tao[1,2], Q. Lu[1,2], S. Wang[1,2], and L. Dai[3]

[1]CAS Key Laboratory of Geospace Environment, Department of Geophysics and Planetary Sciences, University of Science Technology of China, Hefei, Anhui, China, [2]Mengcheng National Geophysical Observatory, School of Earth and Space Sciences, University of Science and Technology of China, Hefei, Anhui, China, [3]School of Physics and Astronomy, University of Minnesota, Twin Cites, Minneapolis, Minnesota, USA

Abstract Effects of magnetic field configuration on the day-night asymmetry of chorus occurrence rate are investigated using a recently developed hybrid code. Previous observational studies show that dayside chorus occurs in regions where the background magnetic field is nearly homogeneous; these observations suggest that the magnetic field configuration might play a significant role in the dayside chorus excitation. In this work, we use a hybrid code to numerically study the threshold conditions of hot electron distributions required to excite chorus waves for different background magnetic field inhomogeneities. Our numerical experiments demonstrate that in a magnetic field with smaller inhomogeneity, smaller temperature anisotropy and smaller number density of hot electrons are needed to excite chorus waves. This conclusion could help explain the higher occurrence rate of chorus waves on the dayside compared with that on the nightside especially in quiet times.

1. Introduction

Chorus waves are electromagnetic emissions playing an important role in energetic electron dynamics in the inner magnetosphere [e.g., *Burtis and Helliwell*, 1976; *Horne and Thorne*, 1998]. The spectrogram of chorus waves typically shows a series of discrete, narrowband rising- or falling-tone elements in the whistler mode frequency range [e.g., *Burtis and Helliwell*, 1976]. Chorus waves can cause enhancement of relativistic electron flux in the outer radiation belt via resonant wave-particle interactions [e.g., *Horne et al.*, 2005; *Reeves et al.*, 2013; *Thorne et al.*, 2013; *Mourenas et al.*, 2014]. These waves can also scatter hundreds of eV to a few keV electrons into the loss cone, causing precipitation of energetic electrons and forming diffuse aurora [*Thorne et al.*, 2010] and pancake distributions [*Tao et al.*, 2011].

Understanding the generation and distribution of chorus waves is important to quantify their effects on energetic electron dynamics. The distribution of chorus waves in the terrestrial magnetosphere exhibits a day-night asymmetry, from which the conditions controlling wave generation process can be hinted. The generation of chorus is believed to be related to the temperature anisotropy of energetic electrons [*Tsurutani and Smith*, 1977; *Li et al.*, 2009a]. These anisotropic distributions of electrons can result from adiabatic heating of plasma sheet electrons as they are transported into the inner magnetosphere during substorms. It is thus expected that nightside chorus waves are related to substorm activities. While drifting eastward to the dayside, energetic electrons are scattered into the loss cone by wave-particle interactions and their density is reduced. Nevertheless, several studies [*Burtis and Helliwell*, 1976; *Tsurutani and Smith*, 1977; *Meredith et al.*, 2003; *Li et al.*, 2009b; *Agapitov et al.*, 2013] have demonstrated the high occurrence rate of chorus waves on the dayside, even during quiet times. For example, *Tsurutani and Smith* [1977] noted the relative independence of dayside chorus from magnetic activity and speculated that the generation of high-latitude dayside chorus might be related to the formation of the "minimum-B pockets" caused by solar wind compression. *Li et al.* [2009b] show that the occurrence rate of moderate ($10 < \langle B_w \rangle < 30$ pT) and strong ($30 < \langle B_w \rangle < 100$ pT) chorus waves is much larger on the dayside than that on the nightside especially in the outer magnetosphere, while moderate chorus ($10 < \langle B_w \rangle < 30$ pT) is also present on the dayside during quiet times. Here $\langle B_w \rangle$ is the average root-mean-square wave amplitude.

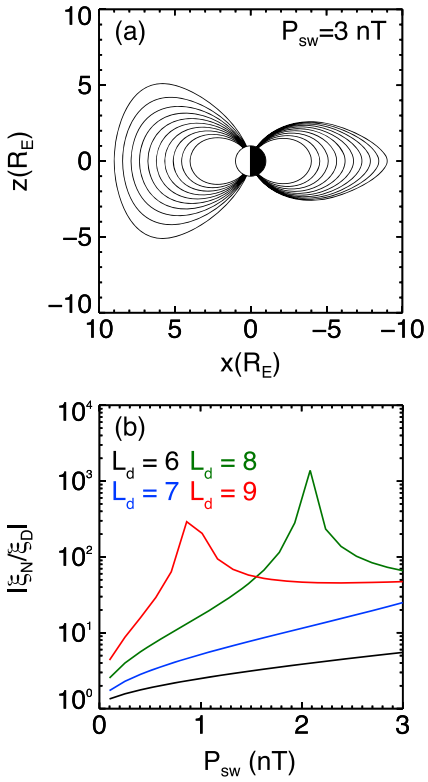

Figure 1. (a) The Earth magnetic field line configuration showing day-night asymmetry calculated using T01 magnetic field model, assuming solar wind pressure $P_{sw} = 3$ nT. (b) The ratio of $|\xi_N/\xi_D|$ as a function of solar wind pressure at different normalized radial distances on the equatorial plane.

To understand the generation of chorus waves on the dayside, *Spasojevic and Inan* [2010] analyzed wave data from two Automatic Geophysical Observatories (AGO) in Antarctica. They found that the occurrence rates of dayside chorus waves appear to be relatively independent of geomagnetic activity but are sensitive to solar wind dynamic pressure. *Spasojevic and Inan* [2010] have considered several possible factors that might contribute to the excitation of chorus on the dayside. These factors include the formation of highly anisotropic electron distributions due to drift shell splitting and the high homogeneity of the background magnetic field due to solar wind compression of the dayside magnetosphere. *Keika et al.* [2012] performed a case study using conjugate observations made by AGO and The Time History of Events and Macroscale Interactions during Substorms (THEMIS) [*Angelopoulos*, 2008]. They found that chorus waves on the dayside occur in a region where the local magnetic field is nearly uniform. Both studies of *Spasojevic and Inan* [2010] and *Keika et al.* [2012] clearly demonstrate the importance of local magnetic field configuration on the generation of chorus.

The motivation of this study is to understand the effects of magnetic field configuration on the day-night asymmetry of chorus occurrence rate. We perform a series of numerical experiments to investigate the threshold conditions of chorus generation using a previously developed hybrid simulation code DAWN [*Tao*, 2014]. The implications of our results on the day-night asymmetric distribution of chorus in the terrestrial magnetosphere and the excitation of chorus waves in other situations will also be discussed.

2. Numerical Model and Simulation Setup

We use a recently developed hybrid code DAWN to simulate the generation of chorus [*Tao*, 2014]. The DAWN code models cold electrons by linearized fluid equations and hot electrons by particle-in-cell techniques [*Birdsall and Langdon*, 2004]. The hot electron distribution is modeled as a bi-Maxwellian with number density n_h. The background magnetic field $\mathbf{B}_0$ has a dominant z component which is parabolic; i.e., $B_{0z}(z) = B_{0z}(0)(1 + \xi z^2)$. Here ξ is the inhomogeneity factor of $\mathbf{B}_0$. An inhomogeneous background magnetic field is believed to be essential to the chorus excitation. For example, *Omura et al.* [2008] suggested that the inhomogeneity of the background magnetic field is important for the formation of currents of resonant particles responsible for chorus wave generation. For the dipole component of a planetary magnetic field near the equatorial plane, $\xi = 4.5/(R_p L_d)^2$, where R_p is the planet radius and L_d is the radial distance on the equatorial plane normalized by R_p [*Helliwell*, 1967]. The x and y components of the background field are chosen so that $\nabla \cdot \mathbf{B} = 0$. The generated chorus waves are parallel propagating only. Successful reproduction of realistic features of chorus elements using the DAWN code has been reported in *Tao* [2014]. For a detailed description of the code, we refer readers to *Tao* [2014].

When setting up the numerical model, we note that the solar wind compresses the field lines on the dayside and stretches the field lines on the nightside, leading to a strong day-night asymmetry in the inhomogeneity of the background magnetic field characterized by ξ. We show magnetic field lines in the noon-midnight meridian plane for a given solar wind dynamic pressure $P_{sw} = 3$ nT in Figure 1a and the ratio of $|\xi_N/\xi_D|$ as

Table 1. Common Simulation Parameters

Parameter	Value
Cell size	$0.05\,c\lvert\Omega_{e0}\rvert^{-1}$
Number of cells	6554
Number of masking cells at each end	300
Time step	$0.02\,\lvert\Omega_{e0}\rvert^{-1}$
Number of time steps	5×10^5
Number of particles per cell	2000
Cold electron plasma frequency ω_{pe}	$5\,\lvert\Omega_{e0}\rvert$
Parallel thermal velocity $w_{\parallel}$	$0.2\,c$

a function of P_{sw} in Figure 1b. Here subscripts "*N*" and "*D*" refer to the nightside and the dayside, respectively. Both magnetic field lines and the ratio of $|\xi_N/\xi_D|$ are calculated using T01 magnetic field model [*Tsyganenko*, 2002]. All T01 input parameters but P_{sw} are set to 0 to emphasize the controlling effect of P_{sw} on the magnetic field configuration. At a given location, the inhomogeneity parameter ξ is calculated by fitting the local magnetic field strength B as a function of the distance s along the field line from the equatorial plane with $|s| \le 1\,R_E$ using $B(s) = B(0)(1+\xi s^2)$ [*Tao et al.*, 2012]. A large solar wind pressure will also form the off-equatorial "minimum-B" pockets in the outer magnetosphere [*Roederer*, 1970], as can be seen in Figure 1a. The formation of the minimum-B pockets on the dayside leads to the nonmonotonic change of $|\xi_N/\xi_D|$ in Figure 1b at $L_d = 8$ and 9 and a negative value of ξ_D, which is the reason to use the absolute value of ξ_N/ξ_D here. As P_{sw} increases from 1 nT to 3 nT, the inhomogeneity parameter ξ_N can be larger than ξ_D by a factor of 4 to more than 10 at $L_d = 7$.

Besides the ξ parameter of the background magnetic field, there are two important plasma parameters of energetic electrons that show strong day-night asymmetry. One is the energetic electron number density n_h and the other is the energetic electron temperature anisotropy A. The scattering of electrons into the atmosphere by wave-particle interactions as electrons drift from nightside to dayside causes a decrease in n_h on the dayside. At the same time, other factors, like drift shell splitting, lead to an increase in electron temperature anisotropy on the dayside. Therefore, as a very crude model, we have $A_N < A_D$ and $n_{h,N} > n_{h,D}$. To isolate the effects of the hot electron number density and the temperature anisotropy, we will perform two sets of simulations. In each set, we will fix one parameter and vary the other.

The common parameters for all simulations done in this work are shown in Table 1. Note that in order to save computation time, we do not use realistic values of ξ of the terrestrial magnetosphere. Instead, we use a simulation system that is scaled down in size. Two different ξ's are used to represent the dayside and the nightside magnetic field in this work. For dayside magnetosphere, we use $\xi_D = 2.16\times10^{-5}\,c^{-2}\Omega_{e0}^2$, which corresponds to the dipole field of a virtual planet with $R_p = R_E/4$ at $L_d = 8$. For nightside magnetosphere, we use $\xi_N = 4\xi_D = 8.62\times10^{-5}\,c^{-2}\Omega_{e0}^2$ to represent the day-night asymmetry of the magnetic field. Here c is the speed of light in vacuum and Ω_{e0} is the signed electron cyclotron frequency on the equatorial plane ($z = 0$). Please note that when discussing dayside or nightside simulation results in the next section, we refer to those of this virtual planet with $R_p = R_E/4$.

3. Simulation Results

3.1. Fixed n_h and Varying Temperature Anisotropy A

In this section, we set the hot electron number density to be $n_h = 0.6\%\,n_c$ and vary only its temperature anisotropy in both dayside and nightside cases. Subscripts "*h*" and "*c*" refer to hot and cold electrons, respectively. In order to find the threshold temperature anisotropy to excite chorus waves, we perform a series of simulations for a given ξ. Starting from a relatively small temperature anisotropy, we increase A by increasing perpendicular thermal velocity $w_\perp$ by $0.02\,c$ in each simulation. The threshold temperature anisotropy is obtained when a discrete chorus element is observed in the simulation.

Figures 2a and 2b show the frequency-time spectrograms of the generated wave field on the dayside for $A = 1.72$ ($w_\perp = 0.33\,c$) and 2.06 ($w_\perp = 0.35\,c$), respectively. Figures 2c and 2d show the wave spectrograms on the nightside for $A = 5.5$ ($w_\perp = 0.51\,c$) and 6.02 ($w_\perp = 0.53\,c$), respectively. These spectrograms demonstrate that the threshold temperature anisotropy for chorus excitation on the dayside is $A = 2.06$, about 3 times smaller than the threshold temperature anisotropy $A = 6.02$ on the nightside. Hence, a larger ξ requires a larger temperature anisotropy to excite chorus waves if other parameters are fixed.

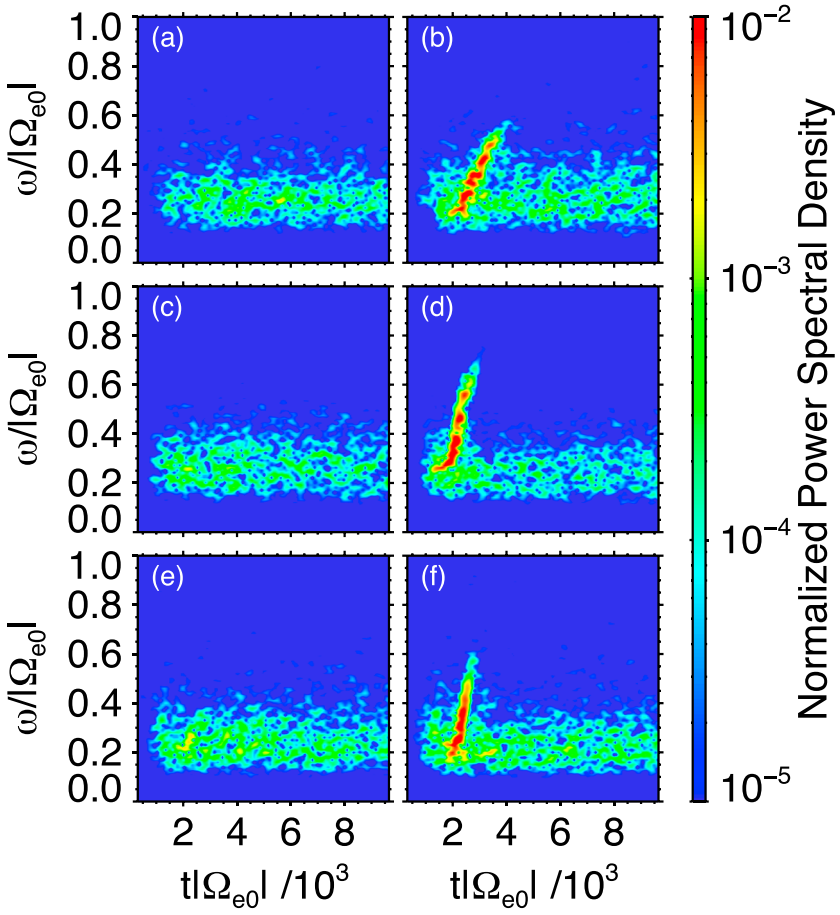

Figure 2. Wave spectrograms for different simulation settings: (a) Dayside case with $A = 1.72$ and $n_h/n_c = 0.6\%$. (b) Dayside case with $A = 2.06$ and $n_h/n_c = 0.6\%$. (c) Nightside case with $A = 5.5$ and $n_h/n_c = 0.6\%$. (d) Nightside case with $A = 6.02$ and $n_h/n_c = 0.6\%$. (e) Nightside case with $A = 2.06$ and $n_h/n_c = 1.36\%$. (f) Nightside case with $A = 2.06$ and $n_h/n_c = 1.53\%$.

3.2. Fixed *A* and Varying Hot Electron Number Density n_h

In this section, we fix the temperature anisotropy $A = 2.06$ and vary n_h to find the minimum hot electron number density needed to excite chorus. We use the nightside case here as an example to illustrate how we perform our simulations. First, we find a value of $n_h = n_{h0}$ such that n_{h0} and $A = 2.06$ result in roughly the same maximum linear growth rate [*Kennel and Petschek*, 1966] on the equatorial plane as $n_h = 0.6\%\ n_c$ and $A = 6.02$, because chorus elements can be generated with $n_h = 0.6\%\ n_c$ and $A = 6.02$ in the nightside case as we have shown in section 3.1. The value of n_{h0} for the nightside case is approximately 1.7% n_c. Then we perform a series of simulations where we decrease or increase n_h by 10% of n_{h0} in each simulation to obtain the minimum n_h to excite chorus waves. Figures 2e and 2f show the wave spectrograms for the nightside case with $n_h = 1.36\%\ n_c$ and $n_h = 1.53\%\ n_c$, respectively. So the minimum n_h for chorus excitation is 1.53% n_c for the nightside case.

For the dayside case, chorus elements can be generated with $A = 2.06$ and $n_h = 0.6\%\ n_c$ as we have shown in section 3.1; the value of n_{h0} is 0.6% n_c. Therefore, we can save computation time by only decreasing n_h by 10% n_{h0} in each simulation. No chorus element can be found in the simulation with $n_h = 0.54\%\ n_c$ in the dayside case; the resulting spectrogram is similar to the one shown in Figure 2a. Therefore, the minimum n_h is 0.6% n_c for the dayside case.

By comparing dayside and nightside simulation results, we conclude that a larger inhomogeneity factor requires a higher hot electron number density to excite chorus waves for a given temperature anisotropy.

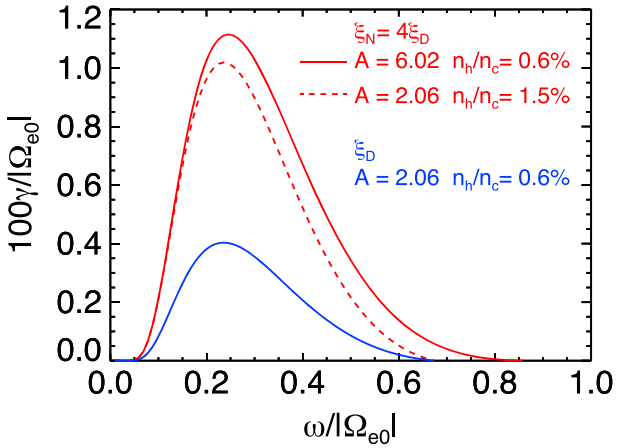

Figure 3. Linear growth rates of whistler waves calculated using the threshold electron distributions on the equatorial plane for dayside and nightside cases. The blue line is for the dayside case ($\xi = \xi_D$) with A= 2.06 and n_h/n_c = 0.6%. Red lines are for the nightside case with $\xi_N = 4\xi_D$. The dashed red line is for A = 2.06 and n_h/n_c = 1.5%; the solid red line is for A = 6.02 and n_h/n_c = 0.6%.

4. Discussion and Summary

In this work, we studied the effects of magnetic field configuration on the day-night asymmetric distribution of chorus occurrence rate by investigating the threshold conditions of chorus excitation. The linear growth rates calculated using those threshold plasma parameters on the equatorial plane are shown in Figure 3. Our major result is that the nearly uniform magnetic field on the dayside significantly lowers the threshold condition of chorus excitation, while the stretched nightside magnetic field requires a higher value of temperature anisotropy or hot electron number density to generate chorus. Based on this result, we conclude that the magnetic field configuration plays an important role in the day-night asymmetry of chorus occurrence rate distribution. Our results can also explain the dependence of dayside chorus occurrence rate on the solar wind pressure observed by *Spasojevic and Inan* [2010], because solar wind pressure has a direct control on the shape of the magnetosphere. In summary, our results suggest that the generation of dayside chorus is a balance between the loss of energetic electrons due to pitch angle scattering caused by wave-particle interactions as electrons drift toward dayside, the enhanced electron temperature anisotropy on the dayside due to drift shell splitting, and the reduced threshold conditions of excitation of chorus due to the smaller inhomogeneity caused by solar wind compression.

One possible physical explanation of our results is that a smaller inhomogeneity factor ξ lowers the threshold wave amplitude that can cause nonlinear phase trapping and phase bunching of electrons [e.g., *Inan et al.*, 1978]. These nonlinear motions of electrons are closely related to the generation of chorus waves. However, unlike emissions triggered by a seeding coherent wave [e.g., *Dysthe*, 1971], chorus wave generation normally involves a linear growth phase when a finite spectrum of whistler waves are excited, as can be seen in Figures 2 and 3. Previous theories about phase trapping and bunching of electrons were developed assuming a coherent wave [e.g., *Dysthe*, 1971]. Therefore, we cannot directly apply those theories to derive quantitatively the threshold wave amplitude of chorus generation without any justification. We leave the investigation of this problem a subject of future work.

Finally, it should be noted that although we started this work to understand the day-night asymmetric distribution of terrestrial chorus occurrence rate, our conclusions also have implications for chorus wave generation in other situations. One example is the generation of whistler waves at magnetotail dipolarization fronts [*Panov et al.*, 2013; *Viberg et al.*, 2014]. It would be interesting to investigate whether discrete chorus elements are present using high-resolution wave data and how the occurrence of chorus waves, if present, is related to the change of local magnetic field inhomogeneity. Another one is the chorus wave generation at other planets, e.g., Saturn [*Hospodarsky et al.*, 2008]. The radius of Saturn is about 10 times larger than the radius of Earth, i.e., $R_S \approx 10\,R_E$. On the equatorial plane, $B_S(r = R_S) \approx B_E(r = R_E)$. Here subscripts "*S*" and "*E*" refer to Saturn and Earth, respectively. If we approximate the inner magnetic field of both planets by a dipole field, then at a given L shell, $\xi_S \approx \xi_E/100$. Provided that other plasma conditions at the two planets are similar, the minimum free energy required to excite chorus at Saturn should be smaller than that needed at Earth. This difference in the threshold conditions of chorus excitation should be verifiable by observations made at Saturn and Earth.

Acknowledgments

This work was supported by USTC grant KY2080000018, NSFC grant 41121003, and CAS Key Research Program KZZD-EW-01-4. The model data will be preserved on a long-term storage system and will be made available upon request to the corresponding author.

Benoit Lavraud thanks two anonymous reviewers for their assistance in evaluating this paper.

References

Agapitov, O., A. Artemyev, V. Krasnoselskikh, Y. V. Khotyaintsev, D. Mourenas, H. Breuillard, M. Balikhin, and G. Rolland (2013), Statistics of whistler-mode waves in the outer radiation belt: Cluster STAFF-SA measurements, *J. Geophys. Res. Space Physics*, *118*, 3407–3420, doi:10.1002/jgra.50312.

Angelopoulos, V. (2008), The THEMIS mission, *Space Sci. Rev.*, *141*, 5–34, doi:10.1007/s11214-008-9336-1.
Birdsall, C. K., and A. B. Langdon (2004), *Plasma Physics via Computer Simulation, Ser. in Plasma Phys.*, 1st ed., Taylor and Francis, New York.
Burtis, W. J., and R. A. Helliwell (1976), Magnetospheric chorus: Occurrence patterns and normalized frequency, *Planet. Space Sci.*, *24*(11), 1007–1010, doi:10.1016/0032-0633(76)90119-7.
Dysthe, K. B. (1971), Some studies of triggered whistler emissions, *J. Geophys. Res.*, *76*(28), 6915–6931.
Helliwell, R. A. (1967), A theory of discrete VLF emissions from the magnetosphere, *J. Geophys. Res.*, *72*(19), 4773–4790.
Horne, R. B., and R. M. Thorne (1998), Potential waves for relativistic electron scattering and stochastic acceleration during magnetic storms, *Geophys. Res. Lett.*, *25*(15), 3011–3014.
Horne, R. B., et al. (2005), Wave acceleration of electrons in the Van Allen radiation belts, *Nature*, *437*, 227–230, doi:10.1038/nature03939.
Hospodarsky, G. B., T. F. Averkamp, W. S. Kurth, D. A. Gurnett, J. D. Menietti, O. Santoík, and M. K. Dougherty (2008), Observations of chorus at Saturn using the Cassini radio and plasma wave science instrument, *J. Geophys. Res.*, *113*, A12206, doi:10.1029/2008JA013237.
Inan, U. S., T. F. Bell, and R. A. Helliwell (1978), Nonlinear pitch angle scattering of energetic electrons by coherent VLF waves in the magnetosphere, *J. Geophys. Res.*, *83*(A7), 3235–3253.
Keika, K., M. Spasojevic, W. Li, J. Bortnik, Y. Miyoshi, and V. Angelopoulos (2012), PENGUIn/AGO and THEMIS conjugate observations of whistler mode chorus waves in the dayside uniform zone under steady solar wind and quiet geomagnetic conditions, *J. Geophys. Res.*, *117*, A07212, doi:10.1029/2012JA017708.
Kennel, C. F., and H. E. Petschek (1966), Limit on stably trapped particle fluxes, *J. Geophys. Res.*, *71*(1), 1–28.
Li, W., R. M. Thorne, V. Angelopoulos, J. W. Bonnell, J. P. McFadden, C. W. Carlson, O. LeContel, A. Roux, K. H. Glassmeier, and H. U. Auster (2009a), Evaluation of whistler-mode chorus intensification on the nightside during an injection event observed on the THEMIS spacecraft, *J. Geophys. Res.*, *114*, A00C14, doi:10.1029/2008JA013554.
Li, W., R. M. Thorne, V. Angelopoulos, J. Bortnik, C. M. Cully, B. Ni, O. LeContel, A. Roux, U. Auster, and W. Magnes (2009b), Global distribution of whistler-mode chorus waves observed on the THEMIS spacecraft, *Geophys. Res. Lett.*, *36*, L09104, doi:10.1029/2009GL037595.
Meredith, N. P., R. B. Horne, R. M. Thorne, and R. R. Anderson (2003), Favored regions for chorus-driven electron acceleration to relativistic energies in the Earth's outer radiation belt, *Geophys. Res. Lett.*, *30*(16), 1871, doi:10.1029/2003GL017698.
Mourenas, D., A. V. Artemyev, O. V. Agapitov, and V. Krasnoselskikh (2014), Consequences of geomagnetic activity on energization and loss of radiation belt electrons by oblique chorus waves, *J. Geophys. Res. Space Physics*, *119*, 2775–2796, doi:10.1002/2013JA019674.
Omura, Y., Y. Katoh, and D. Summers (2008), Theory and simulation of the generation of whistler-mode chorus, *J. Geophys. Res.*, *113*, A04223, doi:10.1029/2007JA012622.
Panov, E. V., A. V. Artemyev, W. Baumjohann, R. Nakamura, and V. Angelopoulos (2013), Transient electron precipitation during oscillatory BBF braking: THEMIS observations and theoretical estimates, *J. Geophys. Res. Space Physics*, *118*, 3065–3076, doi:10.1002/jgra.50203.
Reeves, G. D., et al. (2013), Electron acceleration in the heart of the Van Allen radiation belts, *Science*, *341*(6149), 991–994, doi:10.1126/science.1237743.
Roederer, J. G. (1970), *Dynamics of Geomagnetically Trapped Radiation, Phys. Chem. in Space*, vol. 2, Springer, Berlin, Germany.
Spasojevic, M., and U. S. Inan (2010), Drivers of chorus in the outer dayside magnetosphere, *J. Geophys. Res.*, *115*, A00F09, doi:10.1029/2009JA014452.
Tao, X. (2014), A numerical study of chorus generation and the related variation of wave intensity using the DAWN code, *J. Geophys. Res. Space Physics*, *119*, 3362–3372, doi:10.1002/2014JA019820.
Tao, X., R. M. Thorne, W. Li, B. Ni, N. P. Meredith, and R. B. Horne (2011), Evolution of electron pitch-angle distributions following injection from the plasma sheet, *J. Geophys. Res.*, *116*, A04229, doi:10.1029/2010JA016245.
Tao, X., W. Li, J. Bortnik, R. M. Thorne, and V. Angelopoulos (2012), Comparison between theory and observation of the frequency sweep rates of equatorial rising tone chorus, *Geophys. Res. Lett.*, *39*, L08106, doi:10.1029/2012GL051413.
Thorne, R. M., B. Ni, X. Tao, R. B. Horne, and N. P. Meredith (2010), Scattering by chorus waves as the dominant cause of diffuse auroral precipitation, *Nature*, *467*, 943–946, doi:10.1038/nature09467.
Thorne, R. M., et al. (2013), Rapid local acceleration of relativistic radiation-belt electrons by magnetospheric chorus, *Nature*, *504*, 411–414, doi:10.1038/nature12889.
Tsurutani, B. T., and E. J. Smith (1977), Two types of magnetospheric ELF chorus and their substorm dependences, *J. Geophys. Res.*, *82*(32), 5112–5128, doi:10.1029/JA082i032p05112.
Tsyganenko, N. A. (2002), A model of the near magnetosphere with a dawn-dusk asymmetry 2. Parameterization and fitting to observations, *J. Geophys. Res.*, *107*(A8), SMP 10-1–SMP 10-17, doi:10.1029/2001JA000220.
Viberg, H., Y. V. Khotyaintsev, A. Vaivads, M. André, H. S. Fu, and N. Cornilleau-Wehrlin (2014), Whistler mode waves at magnetotail dipolarization fronts, *J. Geophys. Res. Space Physics*, *119*, 2605–2611, doi:10.1002/2014JA019892.